International Journal of Pharmaceutics 395 (2010) 260–265

Contents lists available at ScienceDirect

International Journal of Pharmaceutics

journal homepage: www.elsevier.com/locate/ijpharm

Pharmaceutical Nanotechnology

Liquid antisolvent preparation of amorphous cefuroxime axetil nanoparticles in a tube-in-tube microchannel reactor

Wen-Zhen Zhu[a,b], Jie-Xin Wang[a], Lei Shao[a,*], Hai-xia Zhang[a], Qian-xia Zhang[a], Jian-Feng Chen[b,**]

[a] Key Laboratory for Nanomaterials, Ministry of Education, Beijing University of Chemical Technology, Beijing, 100029, PR China
[b] Research Center of the Ministry of Education for High Gravity Engineering and Technology, Beijing University of Chemical Technology, Beijing, 100029, PR China

ARTICLE INFO

Article history:
Received 12 November 2009
Received in revised form 9 April 2010
Accepted 14 May 2010
Available online 21 May 2010

Keywords:
Tube-in-tube microchannel reactor
Cefuroxime axetil
Nanoparticles
High throughput
Micromixing

ABSTRACT

This article presents the preparation of nanoparticles of amorphous cefuroxime axetil (CFA) in a microporous tube-in-tube microchannel reactor (MTMCR). The experimental results indicated that CFA particle with a tunable size of 400–1400 nm could be achieved under a high throughput in the range of 1.5–6 L/min. The average particle size decreased with increasing overall volumetric flow rate and decreasing CFA concentration, micropore size, and annular channel width. The produced CFA nanoparticles were characterized by SEM, XRD, FT-IR, DSC and a dissolution test, which indicated that the nanosized CFA was amorphous and exhibited higher dissolution rate compared to the raw CFA. The MTMCR might offer a general and facile pathway for mass production of the nanoparticles of hydrophobic pharmaceuticals thanks to its high throughput capacity and excellent micromixing performance.

1. Introduction

Cefuroxime axetil (CFA) is a poorly water-soluble drug with a high activity against Gram-positive and Gram-negative microorganisms (Crisp and Clayton, 1985; Crisp et al., 1989; Sasinowska et al., 1995). CFA exists as crystalline and amorphous forms, of which the latter shows higher bioavailability and is more desirable. After oral administration, CFA is absorbed and rapidly hydrolyzed by esterases in the intestinal mucosa and portal blood to produce cefuroxime (Crisp et al., 1991; Oszczapowicz et al., 1995). The 1-acetoxyethyl ester group at the position 4 of CFA ensures its lipophilicity and compromises on solubility (Dhumal et al., 2008). Accordingly CFA presents a low solubility and dissolution rate in gastrointestinal tract, which limits its absorption and bioavailability (Chen et al., 2006). Micronization or size reduction is regarded as an effective method to address this problem (Pathak et al., 2004; Perrut et al., 2005).

The traditional micronization methods, such as jet-milling, media milling and high-pressure homogenization (Müllerand and Peters, 1998; Midoux et al., 1999; Merisko et al., 2003), have been attempted to produce drug microparticles. However, these methods need high-energy input and usually result in pharmaceutical contamination, broad particle size distribution and difficulty to control surface properties. Compared to the above methods, liquid antisolvent precipitation (LASP) process (Zhong et al., 2005; Wang et al., 2007; Dong et al., 2009), which is based on the decrease of the solute saturation caused by mixing the solution with an antisolvent, offers an attractive alternative for drug nanoparticle formation at mild temperature and pressure with no requirement of expensive equipment (Li et al., 2007b; Zhao et al., 2007, 2009).

Microtechnology has been attracting attention as a method for the production of fine particles in recent years because of their highly efficient micromixing performance and short transport time, leading to a better control of nucleation and particle growth (Dodge et al., 2004; Lu et al., 2004; Ali et al., 2009). However, due to the structure limitation, the production capacities of most reported microdevice are at μL or mL/min, which are much smaller than those of conventional devices (Nagasawa and Mae, 2006). We have designed and fabricated a high-throughput microporous tube-in-tube microchannnel reactor (MTMCR) to offer a continuous process to produce nanoparticles. The MTMCR demonstrated the excellent micromixing performance and the throughput capacities at L/min level (Wang et al., 2009b), and barium sulphate nanoparticles with an average size of 37 nm and a narrow size distribution were synthesized in the MTMCR (Wang et al., 2009a).

In this study, the MTMCR was employed for the micronization of drugs for the first time. Nanosized CFA was prepared in the MTMCR by LASP. The influence of experimental parameters on CFA nanoparticle formation in the MTMCR was studied and CFA with a particle size of 400–1400 nm was obtained.

* Corresponding author. Tel.: +86 10 64421706; fax: +86 10 64423474.
** Corresponding author. Tel.: +86 10 64446466; fax: +86 10 64434784.
E-mail addresses: shaol@mail.buct.edu.cn (L. Shao), chenjf@mail.buct.edu.cn (J.-F. Chen).

0378-5173/$ – see front matter
doi:10.1016/j.ijpharm.2010.05.018

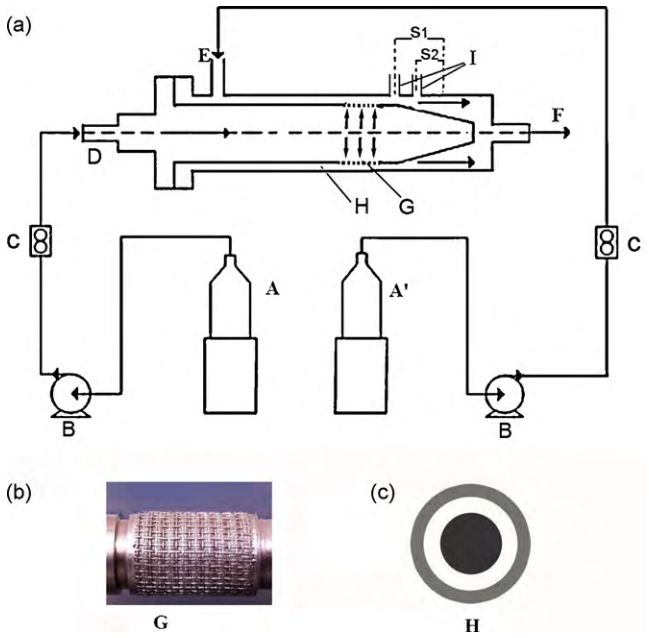

Fig. 1. Experimental setup for the preparation of CFA nanoparticles in a MTMCR. (a) Schematic diagram of experimental setup: A, CFA solution; A′, antisolvent; B, pump; C, flowmeter; D, inlet of inner tube; E, inlet of outer tube; F, outlet; G, micropores; H, annular microchannel; I, sampling points. (b) Photograph of micropore section. (c) Profile of the annular microchannel.

2. Experimental

2.1. Materials and setup

The raw CFA was obtained from North China Pharmaceutical Group Corporation Beta Co., Ltd. (Hebei, China). Acetone and isopropyl ether (A.R. grade) were provided by chemical Agent Co. (Beijing, China).

A schematic diagram of the experimental setup is illustrated in Fig. 1a. Fig. 1b and c shows the micropore section and the profile of the annular microchannel, respectively. Table 1 displays the parameters of the MTMCR used in this study.

2.2. Preparation of CFA

A certain amount of the crystalline raw CFA was dissolved in acetone and filtrated through a 0.22 μm nylon filter to obtain the CFA solution (S). Isopropyl ether (IPE) was employed as the antisolvent (AS). The CFA solution and IPE were pumped into the inner and outer tubes via the inlets D and E, respectively by two magnetic pumps at room temperature. After passing through the micropores radially, the CFA solution was dispersed into microstreams and mixed with IPE in the annular microchannel to precipitate CFA nanoparticles immediately. The slurry was collected at the outlet F and a small amount of the slurry was sampled and diluted in IPE for SEM observation. The other slurry was then filtrated through a 0.22 μm nylon filter, and the filter cake was dried in a vacuum oven at 50 °C for 12 h prior to the characterization.

2.3. Characterization

2.3.1. Particle size and morphology

Particle size and morphology of CFA were observed by scanning electron microscopy (SEM) (JEOL JSM-6360LV). The particle size and its size distribution were generated by the Image-Pro Plus 5.0 via the obtained SEM photographs.

2.3.2. Fourier transform infrared spectrometry (FT-IR)

A FT-IR spectra was recorded with a Bruker IFS-66 spectrometer in the range 450–4000 cm^{-1} using a resolution of 4 cm^{-1} and 16 scans. Samples were grounded with KBr mixing powder and pressed to obtain self-supporting disks.

2.3.3. X-ray diffraction (XRD)

X-ray powder diffraction patterns of the dried CFA samples were obtained using a XRD-6000 diffractometer (Shimadzu, Japan). The powder was placed in a glass sample holder. Cu Kα radiation was generated at 30 mA and 40 kV. Samples of the raw CFA and nanosized CFA were scanned over an angular range of 5–50° with a step size of 0.05°.

2.3.4. Differential scanning calorimetry (DSC)

A DSC (Pyris 1, Perkin-Elmer, USA) was used to obtain DSC thermal profiles of CFA. Samples of raw CFA and nanosized CFA were run at a scanning rate of 10 °C/min. A dry nitrogen purge of 25 mL/min was employed in the process. Calibration of the instrument with respect to temperature and enthalpy was achieved using high purity standard of indium.

2.3.5. High-performance liquid chromatography (HPLC)

The CFA concentration was measured by HPLC (Waters 2965/2996, Miford, MA, USA) with a Waters Sunfire™ C18 reverse-phase column (150 mm × 4.6 mm i.d., 5 μm particle size). The mobile phase was a solution of methanol/(0.2 mol/L aqueous $NH_4H_2PO_4$) 600:400 (v/v). The column was maintained at 30 °C and equilibrated for 60 min with the analytical mobile phase before injection. The injection volume was 50 μL, and the mobile phase was pumped isocratically at a flow rate of 1.0 mL/min. The detection wavelength was 278 nm. The standard curve, whose equation is shown as Eq. (1), was linear (r = 0.999982) in the range from 3 to 60 μg/mL:

$$y = 1.246 \times 10^{-5}x + 0.227 \quad (1)$$

where y is the concentration of CFA, μg/mL, and x is the peak area.

2.3.6. Dissolution test

The dissolution test was carried out using a USP Apparatus 2 (paddle) method (D-800LS, Tianjin, China). The paddle speed and bath temperature were set at 100 rpm and 37.0 ± 0.5 °C, respectively. A 0.1 mol/L HCl solution including 0.1% (w/v) sodium dodecyl

Table 1
MTMCR parameters in this study.

Micropore zone				Non-micropore zone			Other parameters
Material	Micropore size (μm)	Length of micropore zone (mm)	Porosity (%)	Material	Outer tube diameter (mm)	Inner tube diameter (mm)	Throughput (L/min)
Metal meshes	5 –80	1	46	Stainless-steel	15.5 –18	15	1.5 –6

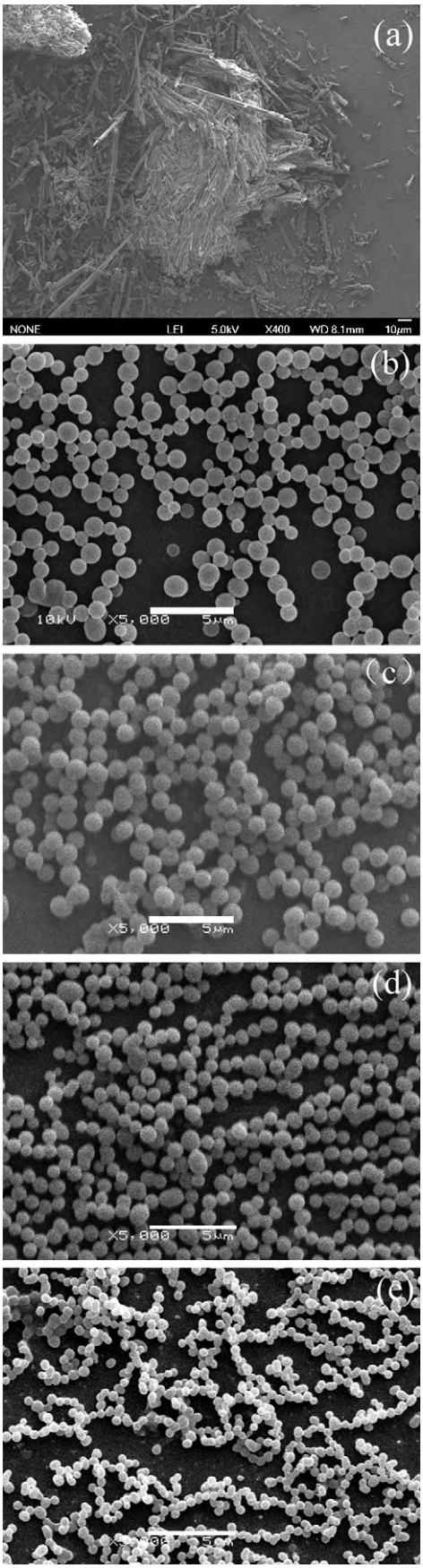

Fig. 2. SEM images of the raw CFA (a) and the nanosized CFA (b–e) prepared at different CFA concentrations. (a) Raw CFA; (b) 20 g/ml; (c) 15 g/ml; (d) 10 g/ml; (e) 5 g/ml. (S/AS: 20; micropore size: 5 μm; channel width: 0.5 mm; overall volumetric flow rate: 6.0 L/min; *T*: 25 °C.)

sulphate was employed as a dissolution medium. 20 mg of CFA was placed into vessels containing 900 mL of the dissolution medium. A 5 mL aliquot of samples was withdrawn from the vessels at an interval of 20 min and filtrated through a 0.45 μm filter. The filtrates were then analyzed by HPLC to determine CFA concentration. Each sample was analyzed in triplicate.

3. Results and discussion

3.1. Effect of the CFA concentration

Fig. 2 shows SEM images of the raw CFA and the nanosized CFA prepared at different CFA concentrations. Compared with the raw CFA (Fig. 2a), the as-prepared CFA (Fig. 2b–e) exhibited a smooth, spherical morphology, good dispersion and smaller particle size, whereas the raw CFA powder had an irregular morphology and a broad particle size distribution, ranging from 2 to 100 μm.

The average CFA particle size (d_p) decreased from 870 nm to 400 nm as the CFA concentration in acetone decreased from 0.20 to 0.05 g/ml. At higher concentration, a larger number of nuclei formed in the A/AS solution, which led to particle aggregation and the formation of larger nanoparticles. In addition, the viscosity of drug solution increased with the increase of the concentration, which hindered the diffusion of the drug from the solution to the antisolvent and resulted in nonuniform supersaturation (Zhang et al., 2009), leading to a large size and broad particle size distribution.

3.2. Effect of the overall volumetric flow rate

Fig. 3 exhibits the influence of the overall volumetric flow rate (Q), which means the sum of the solution flow rate and the antisolvent flow rate, and the corresponding Reynolds (Re) numbers on the average particle size of CFA. The particle size decreased from 760 nm to 440 nm with the increase of the overall volumetric flow rate from 1.5 to 6 L/min. As the overall volumetric flow rate increased, Re increased accordingly, resulting in a stronger turbulence and better micromixing effects between the CFA solution and the antisolvent, which led to a smaller CFA particle size and more uniform particle size distribution (Chen et al., 2005; Wang et al., 2009b).

3.3. Effect of micropore size

Fig. 4 displays the effect of the micropore size on the particle size and the size distribution of CFA. It can be seen that the particle size and distribution were substantially influenced by the micropore size. The CFA particle had a mean size of about 1000 nm with a broad size distribution at a micropore size of 80 μm, whereas the mean particle size significantly decreased to 420 nm with a narrower size distribution as the micropore size decreased to 5 μm. The decrease of the particle size can be explained by the obvious enhancement of the micromixing between the solution and the antisolvent due to the smaller liquid streams of the solution and the larger interfacial area between the dispersed and continuous phases as a result of the decrease of the pore size (Li et al., 2007a).

3.4. Effect of annular channel width

Fig. 5 shows that the annular channel width is anther important parameter for the preparation of the CFA nanoparticles in the

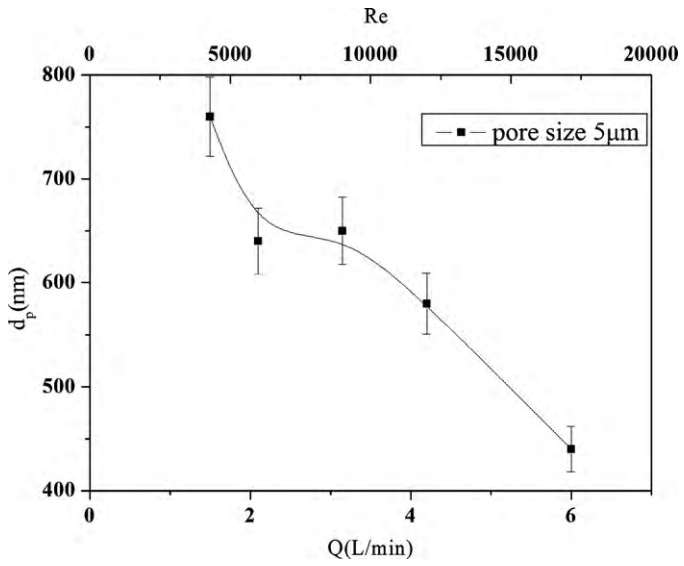

Fig. 3. Influence of the overall volumetric flow rate and Reynolds (Re) number on CFA particle size.

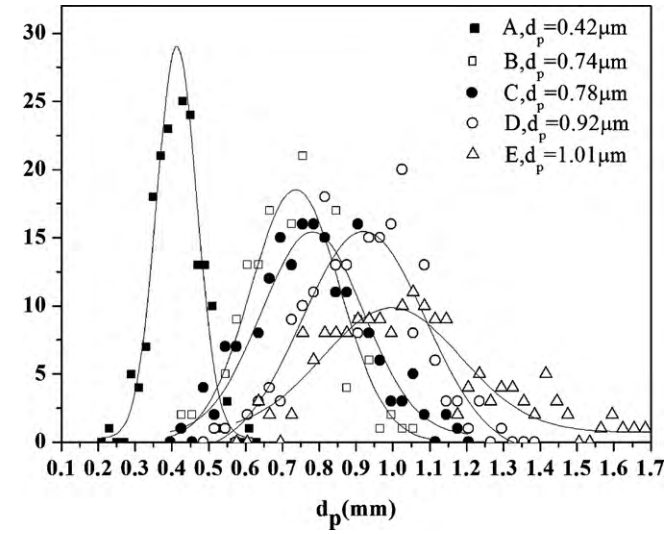

Fig. 4. CFA size and size distribution at different micropore sizes: (A) 5 μm; (B) 10 μm; (C) 20 μm; (D) 40 μm; (E) 80 μm.

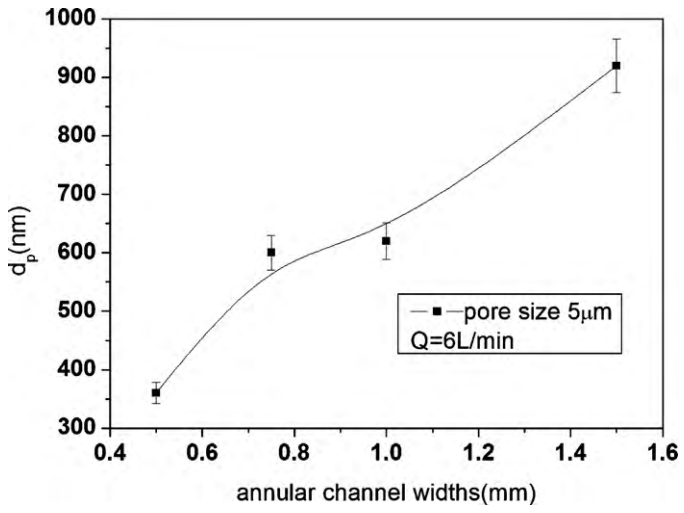

Fig. 5. Size distribution of CFA nanoparticles at different annular channel widths: (A) 0.50 mm; (B) 0.75 mm; (C) 1.00 mm; (D) 1.50 mm.

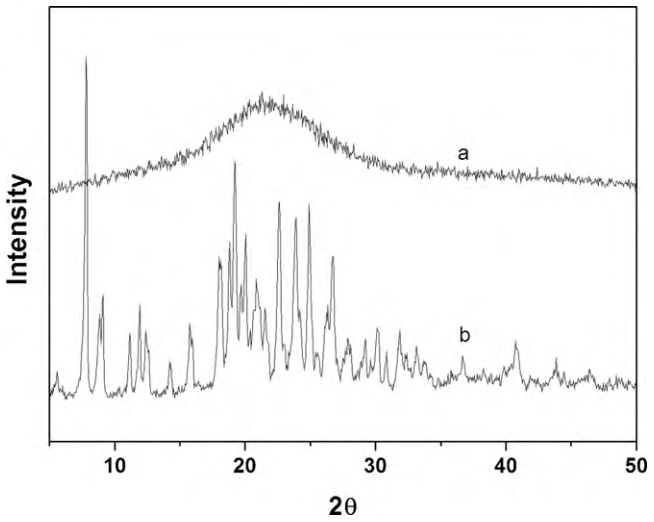

Fig. 6. XRD patterns of (a) raw CFA and (b) nanosized CFA.

MTMCR. When the annular channel width decreased from 1500 μm to 500 μm, the CFA particle size decreased from 920 nm to 360 nm with a narrower particle size distribution. The reason is that the liquid velocity increased with decreasing annular channel width at a certain overall volumetric flow rate of the liquid, thereby resulting in a stronger turbulence and better micromixing effects (Wang et al., 2009a).

3.5. XRD and DSC analyses

The crystalline structure of CFA is assessed by comparing the XRD and DSC profiles of the raw CFA and nanosized CFA. Fig. 6 shows XRD patterns of the raw CFA and the nanosized CFA powder. The raw CFA exhibited some intense crystalline peaks between 5° and 50°. However, only one broad and diffuse peak was detected in the pattern of the nanosized CFA, which indicated that the as-prepared nanosized CFA was in the desired amorphous form. This finding was confirmed by comparing the DSC thermal profile of the raw CFA and nanosized CFA (Fig. 7). There were two endothermic bands around 125 °C and 180 °C for the raw CFA, which indicated that the raw CFA was in polymorphs. In contrast, only one endothermic band around 87 °C with lower enthalpy was present

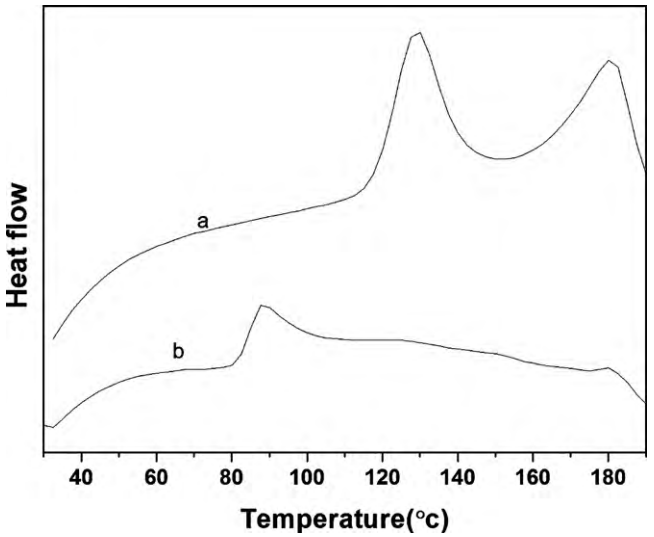

Fig. 7. DSC curves of (a) raw CFA and (b) nanosized CFA.

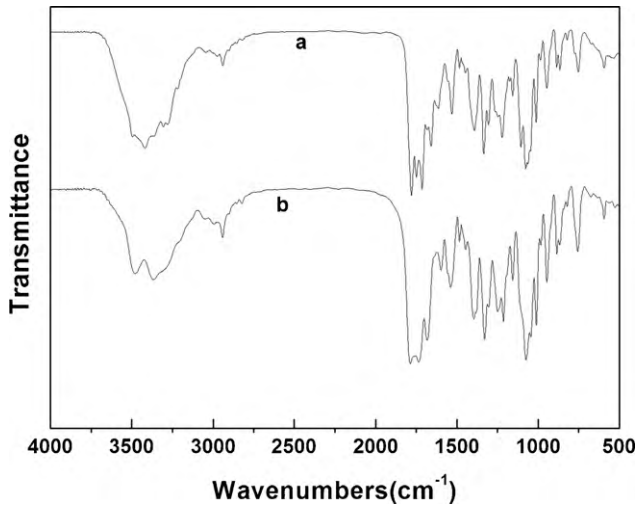

Fig. 8. FT-IR spectra of (a) raw CFA and (b) nanosized CFA.

for nanosized CFA, confirming that the nanosized CFA was mainly in amorphous form.

3.6. FT-IR spectroscopy

FT-IR spectra of the raw CFA and the nanosized CFA in the range of 500–4000 cm^{-1} are presented in Fig. 8. The spectra of the CFAs are characterized by the NH, NH_2 complex (3480–3210 cm^{-1}), β-lactam (1782 cm^{-1}), acetate (1760 cm^{-1}), 4-ester group (1720 cm^{-1}) and 7-amido (1676 and 1534 cm^{-1}). The identical FT-IR spectra curves of the raw CFA and the nanosized CFA suggested that there was no change in the CFA molecular structure after micronization.

3.7. Dissolution test

Fig. 9 depicts the dissolution rates of the raw CFA and the as-prepared nanosized CFA. The nanosized CFA reached a dissolution percentage of 82% within 40 min, whereas only 46% of the raw CFA dissolved during the same period. During the 100 min testing period, about 95% of the nanosized CFA dissolved, but only 57% of the raw CFA dissolved. The results indicated that the nanosized CFA exhibited better dissolution properties than did the raw CFA. Because no surfactants were added into the raw CFA and the nanosized CFA, the increased dissolution rate of the nanosized CFA was attributed to the significant reduction of the particle size and the corresponding increase of the specific surface area. Therefore, LASP in the MTMCR is an effective approach for decreasing particle size to enhance the solubility of poorly water-soluble drugs.

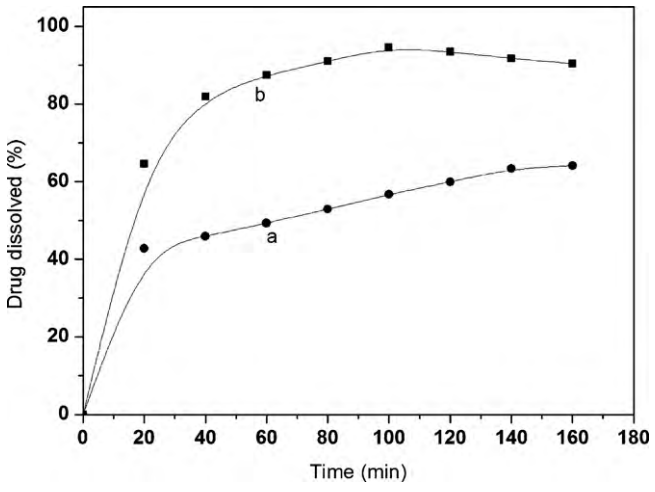

Fig. 9. Dissolution profiles of (a) raw CFA and (b) nanosized CFA.

4. Conclusions

This study provides an alternative methodology for the preparation of the nanoparticles of poorly water-soluble drugs by using a tube-in-tube microchannel reactor (MTMCR). The CFA nanoparticles with an average size of 400 nm could be obtained at a high throughput of 6 L/min. The particle size and the size distribution of the as-prepared CFA particle spheres can be tuned by regulating the experimental parameters, such as the overall volumetric flow rate, the CFA concentration, the micropore size, and the annular channel width. The average particle size of CFA decreased with increasing overall volumetric flow rate and decreasing CFA concentration, micropore size and annular channel width. In addition, the small size of the amorphous CFA nanoparticles led to a significant boost of the dissolution rate. These results indicate that the MTMCR shows potentials for industrial application owing to the excellent micromixing performances and the high throughput capacity.

Acknowledgements

This work was supported by the National "863" Program of China (Nos. 2007AA030207 and 2009AA033301), the National Natural Science Foundation of China (Nos. 20806004 and 20821004), and the Program for New Century Excellent Talents in University of China (NCET-07-0053).

References

Ali, H.S.M., Yorka, P., Blagdena, N., 2009. Preparation of hydrocortisone nanosuspension through a bottom-up nanoprecipitation technique using microfluidic reactors. Int. J. Pharm. 375, 107–113.
Chen, G.G., Luo, G.S., Li, S.W., Xu, J.H., Wang, J.D., 2005. Experimental approaches for understanding mixing performance of a minireactor. AIChE J. 51, 2923–2929.
Chen, J.F., Zhang, J.Y., Shen, Z.G., Zhong, J., Yun, J., 2006. Preparation and characterization of amorphous cefuroxime axetil drug nanoparticles with novel technology: high-gravity antisolvent precipitation. Ind. Eng. Chem. Res. 45, 8723–8727.
Crisp, H.A., Clayton, J.C., 1985. Amorphous form of cefuroxime ester. US Patent. 4,562,181.
Crisp, H.A., Clayton, J.C., Elliott, L.G., Wilson, E.M., 1989. Preparation of a highly pure, substantially amorphous form of cefuroxime axetil. US Patent 4,820,833.
Crisp, H.A., Clayton, J.C., Elliott, L.G., Wilson, E.M., 1991. Process for preparing cefuroxime axetil. US Patent 5,013,833.
Dhumal, R.S., Biradar, S.V., Yamamura, S., Paradkar, A.R., York, P., 2008. Preparation of amorphous cefuroxime axetil nanoparticles by sonoprecipitation for enhancement of bioavailability. Eur. J. Pharm. Biopharm. 70, 109–115.
Dodge, A., Jullien, M.C., Lee, Y.K., Niu, X., Okkels, F., Tabeling, P., 2004. An example of a chaotic micromixer: the cross-channel micromixer. C. R. Phys. 5, 557–563.
Dong, Y.C., Ng, W.K., Shen, S.C., Kim, S.G., Tan, R.B.H., 2009. Preparation and characterization of spironolactone nanoparticles by antisolvent precipitation. Int. J. Pharm. 375, 84–88.
Li, S.W., Xu, J.H., Wang, Y.J., Luo, G.S., 2007a. Mesomixing scale controlling and its effect on micromixing performance. Chem. Eng. Sci. 62, 3620–3624.
Li, X.S., Wang, J.X., Shen, Z.G., Zhang, P.Y., Chen, J.F., Yun, J., 2007b. Preparation of uniform prednisolone microcrystals by a controlled microprecipitation method. Int. J. Pharm. 342, 26–32.
Lu, H., Gaudet, S., Schmidt, M.A., Jensen, K.F., 2004. A microfabricated device for subcellular organelle sorting. Anal. Chem. 76, 5705–5712.
Merisko, L.E., Liversidge, G.G., Cooper, E.R., 2003. Nanosizing: a formulation approach for poorly-water-soluble compounds. Eur. J. Pharmacol. Sci. 18, 113.
Midoux, N., Hosĕk, P., Pailleres, L., Authelin, J.R., 1999. Micronization of pharmaceutical substances in a spiral jet mill. Powder Technol. 104, 113.
Müllerand, R.H., Peters, K., 1998. Nanosuspensions for the formulation of poorly soluble drugs I. Preparation by a size-reduction technique. Int. J. Pharm. 160, 229.
Nagasawa, H., Mae, K., 2006. Development of a new microreactor based on annular microsegments for fine particle production. Ind. Eng. Chem. Res. 45, 2179–2186.
Oszczapowicz, I., Malafiej, E., Szelachowska, M., Horoszewicz-Malafiej, A., Kuklewicz, C., Sieranska, E., Denys, A., Niedworok, J., 1995. Esters of cephalosporins.

Part II. Differences in the properties of various forms of the 1-acetoxyethyl ester of cefuroxime. Acta Pol. Pharm. Drug Res. 52, 397–401.
Pathak, P., Meziani, M.J., Desai, T., Sun, Y.P., 2004. Nanosizing drug particles in supercritical fluid processing. J. Am. Chem. Soc. 126, 10842–10843.
Perrut, M., Jung, J., Leboeuf, F., 2005. Enhancement of dissolution rate of poorly soluble active ingredients by supercritical fluid processes. Part I: micronization of neat particles. Int. J. Pharm. 288, 3–10.
Sasinowska, M., Winiewska, I., Gumulka, W., Oszczapowicz, I., Szelachowska, M., Interewiez, B., 1995. Esters of cephalosporins. Part I. Permeability of cefuroxime liberated from its 1-acetoxyethyl ester through biological membranes: influence of the form and size of the ester particles. Acta Pol. Pharm. Drug Res. 52, 397–401.
Wang, Q.A., Wang, J.X., Li, M., Shao, L., Chen, J.F., Gu, L., An, Y.T., 2009a. Large-scale preparation of barium sulphate nanoparticles in a high-throughput tube-in-tube microchannel reactor. Chem. Eng. J. 149, 473–478.
Wang, Q.A., Wang, J.X., Yu, W., Shao, L., Chen, G.Z., Chen, J.F., 2009b. Investigation of micromixing efficiency in a novel high-throughput microporous tube-in-tube microchannel reactor. Ind. Eng. Chem. Res. 48, 5004–5009.
Wang, Z., Chen, J.F., Le, Y., Shen, Z.G., Yun, J., 2007. Preparation of ultrafine beclomethasone dipropionate drug powder by antisolvent precipitation. Ind. Eng. Chem. Res. 46, 4839–4845.
Zhang, H.X., Wang, J.X., Zhang, Z.B., Le, Y., Shen, Z.G., Chen, J.F., 2009. Micronization of atorvastatin calcium by antisolvent precipitation process. Int. J. Pharm. 374, 106–113.
Zhao, H., Wang, J.X., Wang, Q.A., Chen, J.F., Yun, J., 2007. Controlled liquid antisolvent precipitation of hydrophobic pharmaceutical nanoparticles in a microchannel reactor. Ind. Eng. Chem. Res. 46, 8229–8235.
Zhao, H., Wang, J.X., Zhang, H.X., Shen, Z.G., Yun, J., Chen, J.F., 2009. Facile preparation of danazol nanoparticles by high-gravity anti-solvent precipitation method. Chin. J. Chem. Eng. 17, 318–323.
Zhong, J., Shen, Z.G., Yang, Y., Chen, J.F., 2005. Preparation and characterization of uniform nanosized cephradine by combination of reactive precipitation and liquid anti-solvent precipitation under high gravity environment. Int. J. Pharm. 301, 286–293.